11A-06

THE MELTING LAYER OBSERVATION USING A DUAL Ka-BAND RADAR SYSTEM

Kenji Nakamura *
Dokkyo University, Saitama, Japan
Yuki Kaneko
Japan Aerospace Exploration Agency
Katsuhiro Nakagawa, Hiroshi Hanado
National Institute of Information and Communications Technology
and
Masanori Nishikawa
Free

1. INTRODUCTION

The Global Precipitation Measurement (GPM) core satellite carries two instruments for precipitation measurements, that is, a dual-wavelength radar (DPR) and a GPM microwave radiometer (GMI). The GPM covers the whole globe. In a high latitude region, snow frequently falls. Snow rate or equivalent rain rate measurements by radars are more difficult than rain observations, because snow particles have more complicated characteristics of radio scattering than rain drops. In very cold regions, snow is dry, but in slightly warm regions, wet snows more frequently fall. So, the wet snow observations are essential for measurements of global precipitation. The wet snow or a melting layer, which contains partly melted snow particles, has, however, much more complex characteristics in radiowave scattering than dry snow.

The DPR is a 13.6/35.5 GHz radar system. The 35 GHz (Ka-band) spaceborne precipitation radar is a new one. For the full utilization of the 35 GHz radar, radiowave scattering characteristics of precipitation particles must be well understood. In the Ka-band, attenuation of the radiowave is strong, and conventional Ka-band radars measure only the combination of scattering and attenuation. It is important to separate the effects of scattering and attenuation for precise precipitation measurement using Ka-radars. In order to measure scattering and attenuation characteristics of precipitation particles separately, a dual Ka-band radar system (DKR) was developed by JAXA. Some results of melting layer observation are described in this paper.

2. METHOD

DKR consists of two identically designed Ka-band radars. When a precipitation system comes between two radars, the radars observe the precipitation system from opposite directions (Fig. 1). The precipitation echoes in the Ka-band suffer from strong rain attenuation. The reduction due to rain attenuation symmetrically appears in both radar echoes as shown in Fig. 2. By differentiating measured radar reflectivity (Z_{m1}, Z_{m2}) with range, the specific attenuation can be estimated. After obtaining the specific attenuation (k), equivalent radar reflectivity (Ze) is estimated. In the melting layer, specific attenuation and the equivalent radar reflectivity vary largely along the radio path, and the estimated specific attenuation is very sensitive to the setup configuration of the experiment. The accuracy of the estimated specific attenuation was found to depend on the curvature of the profile, that is, the doubly differentiated value of the equivalent radar reflectivity with respect to range and the distance for the differentiation. The accuracy is also limited by natural fluctuation of the precipitation system. The observation has been performed along a mountain

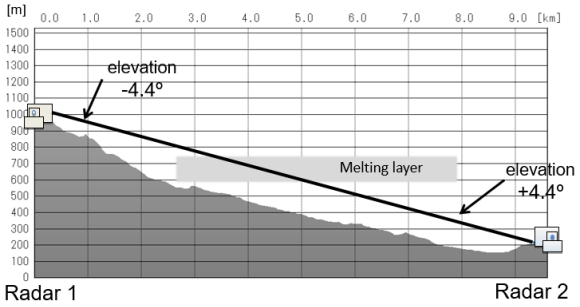

Fig. 1. Configuration of the melting layer observations at Zao Mountain slope

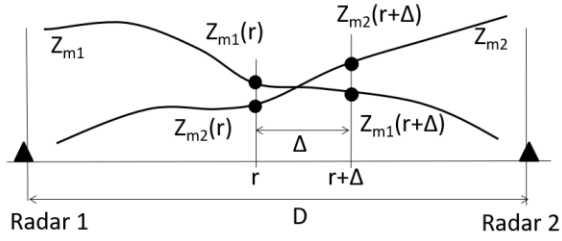

Fig. 2. Schematic illustration of the measured radar reflectivity by DKR.

* *Corresponding author address:* Kenji Nakamura, Dokkyo Univ., Soka, Saitama, Japan, Dept. of Ecomomics, Soka, Saitama 340-0042, Japan; e-mail: k13002@dokkyo.ac.jp

(Mt. Zao) slope and the radio path is near the surface. The height difference between two radars are about 800 m which is sufficient for melting layer observation if melting layer comes well in the range. In this case, precipitation system is likely affected by the topography and have a fine structure, and even a small beam mismatching of the two radars causes unacceptable errors (Nakamura et al. 2018). In order to overcome the uncertainty, parameter tuning and selection of strong melting layer observation cases are applied.

3. RESULTS

On 1 March 2015, a strong melting layer appeared. In this day, a melting layer suddenly appeared at 21:15 JST, and disappeared at about 21:40 JST. After that, the melting layer again appeared at about 21:30 JST. The sudden change of the melting layer was also observed by a micro rain radar. Doppler data of DKR also show rapid variation in radial velocity. The meteorological mechanism is not clear, but it may be due to the slope wind in the mountain region. Figure 3 (left) shows the profiles of the measured Z (Zm) and estimated Ze. The Ze is an average of the two Zm's with a constant bias. The profile of Ze is nearly constant from bottom and have a very small peak which indicates the melting layer. Above the peak, Ze decreases, resulting in a shelf-like profile. The right figure shows the profile of k. The k profile has a clear peak in the melting layer.

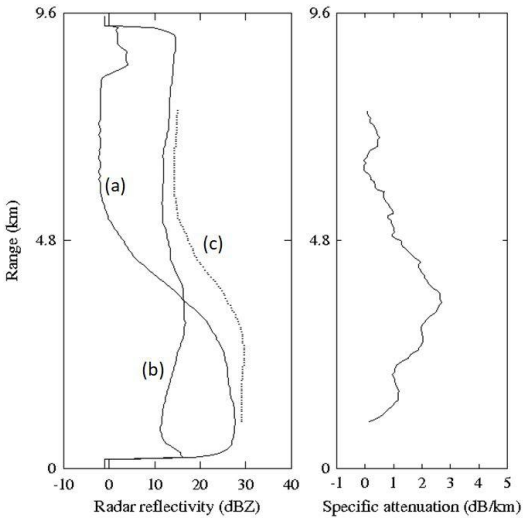

Fig. 3. An example of profiles in rain at the slope of Zao Mountain at 21:28 JST on 1 March 2015. 06:32 (a) in the left figure shows the measured radar .reflectivity of the upper site radar (Radar 1), and (b) is of that of the lower site radar (Radar 2); (c) is the estimated equivalent radar reflectivity. The right figure is the estimated specific attenuation.

To show the relationship between k and Ze, a k-Ze diagram is produced as Fig. 4. Profiles with clear melting layer signatures are chosen to produce the figure. Since the altitude of the melting layer changed, the range is adjusted to have the melting layer at a fixed range. The k-Ze diagram show a loop-shape, that is, during melting, k first increases followed by the increase of Ze. This loop-shape appeared in other melting layer cases, and could be a general characteristic.

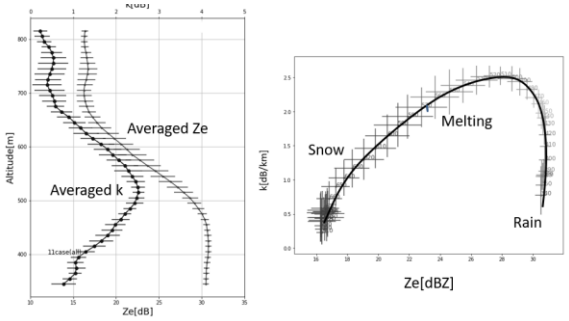

Fig. 4. Averaged k-Ze relationship for data on 1 and 2 March 2015. Left: The profiles of Ze and k relative to the reference height. Right: k-Ze diagram.

4. LOOP-SHAPE IN k-Ze DIAGRAM

Here, we discuss the reasons of the loop-shape. The melting process is complex and the scattering characteristics vary much depending on the details of the melting precipitation particles. Let think a simple sphere particle with given permittivity. The permittivity changes during melting. The size of the particle also changes to reduce to the size of a rain drop. The equivalent relative permittivity of mixed materials which are, in our case, air, ice, and liquid water, is an important parameter. Thought there exist several formula, such as, Maxwell-Garnett model, Gruggeman model (Markel, 2016), or more complex models (Meneghini and Liao, 2000), it still is uncertain. Almost all the reported results, however, show a general characteristics in that the real and imaginary parts of the permittivity changes monotonically with the melting volume ratio. So, we simply assume that the permittivity changes proportionally to the volume ratios of air, ice, and liquid water. The size is another important parameter. By assuming the sphere, the size is determined by the volume melting ratio.

Figure 5 shows relationships between the extinction cross section, σ_e, and backscattering cross sections, σ_b, for a melting snow particle with a raindrop diameter of 1 mm and original snow density of 0.2 g cm^{-3} at 35.5 GHz. Here, the abscissa is in dB. Three curves are shown: (a) Rayleigh calculation with the melted raindrop diameter, (b) Rayleigh calculation with diameter change, and (c) Mie calculation. The curve (a) shows only the effect of the variation of permittivity, and the curve (b) shows the permittivity and size effects. The difference betwenn (a) and (b) is due to the particle size change from a snow particle to a rain drop. The size of the original snow is about 1.7 times greater than the water equivalent raindrop size, corresponding to absorption cross section and scattering cross section which are 5 times and 25

times greater than the water size particles in Rayleigh scattering.

Basic loop-shape is produced by the relative permittivity variation. The large size of the snow particle expands largely the loop. The Mie effect slightly reduces k. The k-Ze diagram also shows a clear peak in the specific attenuation (k). On the other hand, Ze first increases during melting, but reduces only slightly in the last phase of melting, resulting in a shelf-like profile of Ze.

5. SUMMARY.

Equivalent radar reflectivity and specific attenuation in the melting layer are described. It is found that the altitude of the peak of the specific attenuation is slightly higher than that of the equivalent radar reflectivity. The reasons are found due to change of relative permittivity, and change of size of particles. The imaginary part of the permittivity first deceases (more attenuation) followed by increase of the absolute value of the permittivity, which results in a loop-shape k-Ze relationship. The size of the particle decreases during melting. Combined effects of the changes of the permittivity and size cause the basic loop-shape. At the Ka-band, the Mie effect is significant, but in terms of the loop-shape, the Mie effect only slightly modifies the shape.

This kind of study could contribute to improvement of the DPR rain retrieval algorithms, particularly for melting snow or wet snow. There exist several models for the melting layer. Our results may contribute to evaluate the model reliability. Our results are, however, not conclusive. One reason is the uncertainty of the accuracy of the estimation of the equivalent radar reflectivity and specific attenuation, and the other is the observation locations. Observation locations are at the slopes of mountains. The radio path of the radar is separated from the ground by only about 200 m. The ground clutter does not contaminate the radar signature thanks to the narrow beam and well suppressed far sidelobes in the antenna pattern. However, the atmospheric conditions may be different from the free atmosphere. For example, slope winds may destroy the structure of the melting layer.

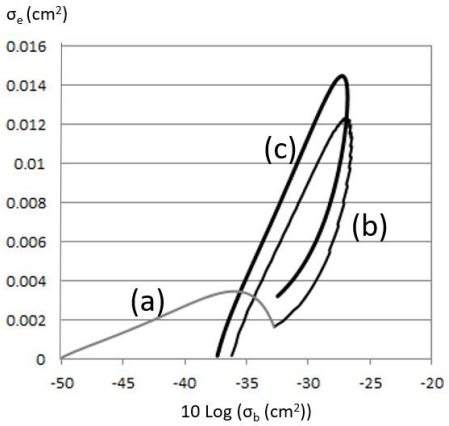

Fig. 5. The relationship between the extinction cross section, σ_e and backscattering cross sections , σ_b for a melting snow particle with a raindrop diameter of 1 mm, 35.5 GHz. (a) Rayleigh calculation with the raindrop diameter, (b) Rayleigh calculation, and (c) Mie calculation.

REFERENCES

Markel, V. A., 2016: Introduction to the Maxwell-Garnett approximation: tutorial. *J. Opt. Soc. Amer.*, 33, 1244-1256, doi:10.1364/JOSSA.33.001244.

Meneghini, R., and L. Liao, 2000: Effective dielectric constants of mixed-phase hydrometeors. *J. Atmos. Oceanic Technol.*, 17, 628-649.

Nakamura et al., 2018: Measurement method for specific attenuation in the melting layer using a dual Ka-band radar system. *IEEE Trans. Geosci. Remote Sens.*, 56, 3511-3519, doi:10.1109/TGRS.201801291.